Langmuir and Langmuir−Blodgett Films of NLO Active 2-(*p*-*N*-Alkyl-*N*-methylamino)benzylidene-1,3-indandione−π/*A* Curves, UV−Vis Spectra, and SHG Behavior

Hanna Schwartz,[†] Royi Mazor,[†] Vladimir Khodorkovsky,*[,†] Lev Shapiro,[†] Jacob T. Klug,[‡] Efim Kovalev,[‡] Guilia Meshulam,[§] Garry Berkovic,[§] Zvi Kotler,[§] and Shlomo Efrima*[,†,∥]

Department of Chemistry, Ben-Gurion University, Beer-Sheva, 84105, Israel, The Institute of Applied Sciences, Ben-Gurion University, Beer-Sheva, 84105, Israel, Photonic Materials Group, Soreq NRC, Yavne, 81800, Israel, and The Ilse Katz Center for Meso and Nanoscale Science and Technology, Ben-Gurion University, Beer-Sheva, 84105, Israel

Received: October 20, 2000; In Final Form: February 14, 2001

We study 2-(*p*-*N*-hexadecyl-*N*-methylamino)benzylidene-1,3-indandione **(1a)** as a model compound for the preparation of nonlinear optically (NLO) active Langmuir−Blodgett (LB) layers. The pressure−area (π−*A*) isotherm of **(1a)** at the air−water interface is investigated. A limiting area of 0.60 ± 0.02 nm^2 per molecule is found. The alternate-layer LB deposition of compound **(1a)** and an inert spacer, cadmium stearate, at different surface pressures is performed. The effects of temperature and delay time between spreading of the Langmuir film and the deposition of the LB films are studied. An increase of collapse pressure from 20 to 30 mN/m is observed as the delay time increases. UV−vis spectra indicate a uniform transfer of **(1a)** and show compression-induced changes as a function of the deposition conditions. A split of the absorption maximum is observed for LB films deposited at higher pressures and lower temperatures. The two bands can result from two different molecular electronic transitions, affected by the aligning influence of the surface, and the different environments in the film compared to solution. Alternatively, these two bands can be associated with (at least) two different conformers. The orientation of the transition moments is evaluated on the basis of polarized UV−vis spectra at different angles of incidence, and found to be 40−44°. Significant second harmonic (SH) generation by the LB films is observed. Analysis of the SH response gives a tilt angle of 44°, in agreement with the finding from UV absorbance.

Introduction

Molecules consisting of a donor (D) moiety linked to an acceptor (A) moiety by a conjugated bridge have become the subject of intensive study due to their potential in NLO applications.[1] The development of advanced materials for photonic applications based on second harmonic generation requires solution of several major problems. The first is the design of donor−(π-bridge)−acceptor chromophores with maximized hyperpolarizabilities that retain reasonable thermal and photostability. Such D−(π-bridge)−A materials may be optimized by varying the donor−acceptor strength and the length of the π-electron bridge.[2] Although significant progress in deriving the structure−properties relationship has been made,[3] full guidelines for the design of SHG chromophores are not yet established. The second problem is the assembly of these chromophores in noncentrosymmetric arrangements in miniaturized nanoscale systems. This can be realized by fabrication of LB (or self-assembled, SA) films incorporating a compatible inert spacer material.[4] The aim of the present work is to study Langmuir and LB films of 2-(*p*-*N*-hexadecyl-*N*-methylamino) benzylidene-1,3-indandione (**1a**), Figure 1, as a model for related

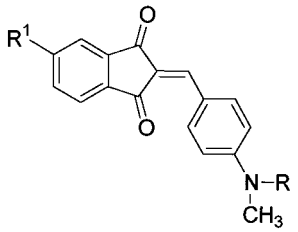

1 a) R = $C_{16}H_{33}$, R^1 = H
b) R = CH_3, R^1 = H
c) R = CH_3, R^1 = $C_{17}H_{35}$
d) R = C_8H_{17}, R^1 = H
e) R = $C_{22}H_{45}$, R^1 = H

Figure 1. 2-(*N*-Methylamino) benzylidene-1,3-indandione and derivatives.

NLO derivatized chromophores. This compound is a simple prototype of a newly developed family of materials consisting of compounds derived from a 1,3-indandione-2-ylidene moiety as an acceptor (A) and a *p*-dimethylaminophenyl moiety as a donor (D). Recently, the photophysical properties of its *N*,*N*-dimethylamino analogue (**1b**) in the solid state (crystals and thin films)[5] have been studied. The 1,3-indandione moiety can also serve in the second role of a hydrophilic headgroup of an amphiphile. Attaching a long-chain substituent (C16, for instance) as the hydrophobic tail, may allow formation of Langmuir films at the water/air interface, as precursors for LB films.

Recently Rutkis et al.[6] studied Langmuir and LB films of the same type of chromophore (**1c**). However, the long chain in their compound was attached at position 5 of the indandione acceptor moiety. In contrast, the molecule we study here has the aliphatic chain attached to the amino group of the donor.

* Corresponding authors. E-mail: hodor@bgumail.bgu.ac.il; efrima@bgumail.bgu.ac.il.
[†] Department of Chemistry, Ben-Gurion University.
[‡] The Institute of Applied Sciences, Ben-Gurion University.
[§] Photonic Materials Group, Soreq NRC.
[∥] The Ilse Katz Center for Meso and Nanoscale Science and Technology, Ben-Gurion University.

10.1021/jp0038916 CCC: $20.00
Published on Web 06/01/2001

Rutkis et al.[6] focused on the phase behavior and the UV−vis spectra of single-component LB films, while we produce alternating LB films (using a spacer) with NLO applications in mind. In addition, it is of interest to compare the effect of the different position of the hydrophobic tail on the surface properties of this molecule. This is a rare opportunity to study such effects. One might expect, for instance, that the orientation of the chromophore with respect to the surface is different in the two cases.

In this report we present the surface properties of Langmuir and LB alternating films of **(1a)**. We also study time and temperature effects. On the basis of UV−vis absorption spectroscopy and SH measurements we discuss the molecular arrangement of **(1)** in the LB films in terms of the tilt angle of the transition moments.

Experimental Section

Compounds **1a, 1d,** and **1e** are synthesized in analogy to the known procedure[7] and are purified by column chromatography on silica gel and subsequent crystallization. Dichloromethane and chloroform are of analytical grade (Frutarom). The spacer is stearic acid (Aldrich, 99%). Water is of ∼18 MΩ cm resistivity, obtained from a Barnsted E-pure water purifier. We use a Labcon Ltd, modular double trough for π/A studies and LB deposition.

Pressure−area isotherms of Langmuir films are obtained by spreading compound **1a** from a CH_2Cl_2 solution (2.25 mg/mL) onto pure water in one compartment of the dual LB trough. A preset curing time in the range 30−120 min is than followed by compression at 1 $cm^2\ s^{-1}$ (ca. 0.15% s^{-1} of the compartment area). The surface pressure/molecular area isotherms are measured in the temperature range 8−22 °C and at pH 5.5 ± 0.5. Control of the temperature is obtained with a refrigerated circulator (Julabo GmbH, Model F12). Similar procedures are used for compounds **1d** and **1e**.

To prepare LB films, compound **1a** is spread as described above in one compartment of the LB trough onto an aqueous 0.03 mM $CdCl_2$ solution. It is relaxed for a prescribed time (30−120 min) and then compressed. The spacer, stearic acid, is spread from a chloroform solution (2.6 mg/mL) in the second compartment of the trough. Alternate-layer films of **(1a)** and the spacer are obtained by the conventional vertical dipping technique. A hydrophobic glass substrate is passed through the floating monolayers at a rate of 0.5 cm min^{-1}. Compound **1a** is deposited in the down stroke at a constant pressure selected in the range 20−40 mN/m, and the spacer is picked up in the subsequent upstroke at 30 mN/m.

Hydrophobic substrates are produced by coating (24 × 50 × 1 mm) glass slides with octyltrichlorosilane (OTS) using the following procedure. The glass slides are first cleaned with piranha solution (H_2SO_4/H_2O_2, 4:1) at 90 °C for 60 min, followed by consecutive water, ethanol, and acetone rinses, and are finally dried in air. Clean substrates are immersed in a 2.5 mM OTS solution in CCl_4 for 1−2 h and then rinsed four times with ethanol.

Absorption spectra of the LB films deposited on glass substrates are taken with a 8452A HP diode array spectrophotometer with a 2 nm resolution. Polarized absorbance spectroscopy is applied at different angles of incidence.

For SHG measurements the films are deposited onto 1 mm thick glass slides at 20mN/m after a 30 min relaxation of the Langmuir film. SH measurements of the LB films are performed using 7 ns 1.064 μm laser pulses ("Surelite II", Continuum) attenuated below 1 mJ and weakly focused on the sample to a spot size of approximately 1 mm. The SH signal is measured in transmission with the sample placed on a rotation stage, enabling the incidence angle of the laser to the sample surface normal to be varied from −65° to 65°. Excitation uses either p- or s-polarized light.

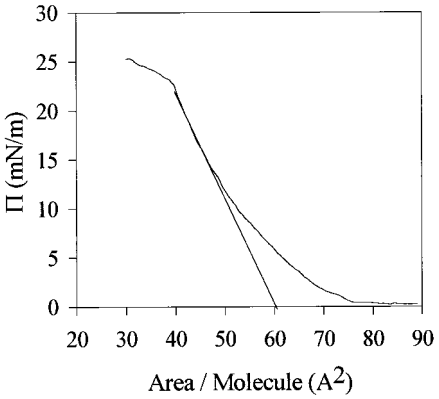

Figure 2. Pressure−area isotherm of compound **(1a)** at 22 °C. The straight line is the extrapolation to zero pressure giving an area of 0.60 nm^2/molecule.

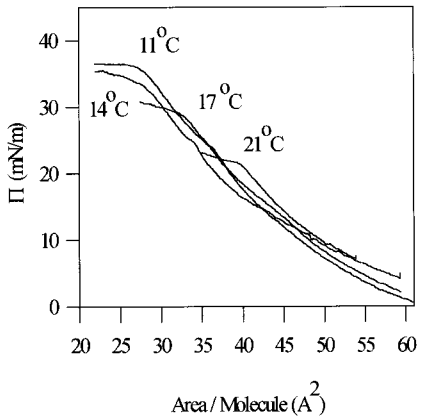

Figure 3. Pressure−area isotherms of compound **(1a)** at different temperatures.

Results and Discussion

***π*−*A* Isotherms.** Compound **1a** forms stable Langmuir monolayers as exhibited by the pressure−area (π/A) isotherms. A typical isotherm (Figure 2) shows an initial characteristic low-pressure liquid-expanded region followed by a liquid-compressed region merging into a solid-condensed region with a limiting me an molecular area of about 0.60 nm^2, obtained by extrapolating the high-pressure region of the isotherm to $\pi = 0$.

The temperature dependence of the $\pi-A$ isotherms of **(1a)** on pure water is shown in Figure 3. The collapse pressure gradually increases with the decreasing temperature and shifts to smaller molecular areas. The increase of the collapse pressure is probably due to the more ordered arrangement of hydrocarbon chains at lower temperatures. Within the uncertainty of our results the molecular areas and surface pressures at which the liquid-extended to liquid-compressed and the liquid-compressed to solid transitions take place are independent of the temperature.

The $\pi-A$ isotherms in the same temperature range are measured using different time delays between the spreading of the film and the recording of the isotherms. An increase of the collapse pressure from 20 to 30 mN/m is observed for longer delay times (Figure 4A,B). A new (unidentified) phase transition

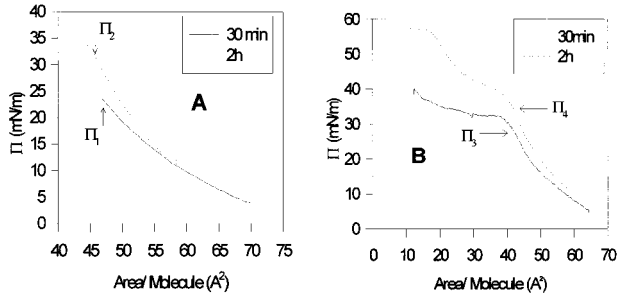

Figure 4. $\pi-A$ isotherms of compound **(1a)** at different delay times (2h, dotted line; 30 min, solid line) and temperatures: (A) 22 °C, (B) 13 °C.

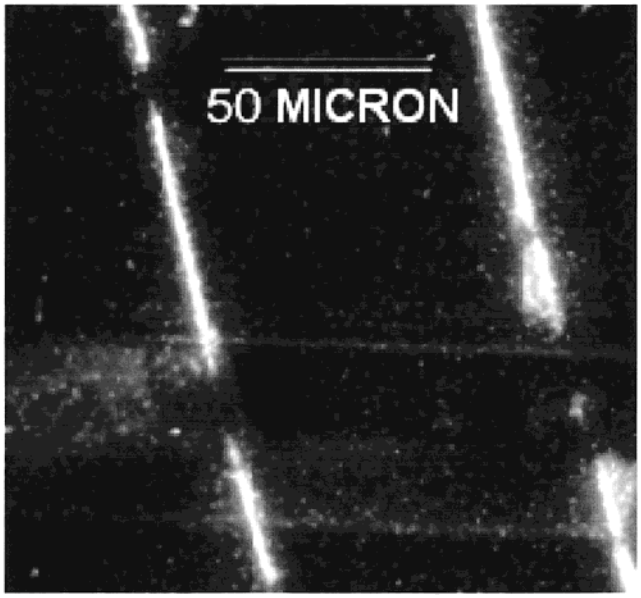

Figure 5. Fluorescence microscopy of collapsed Langmuir monolayer of compound **(1a)**.

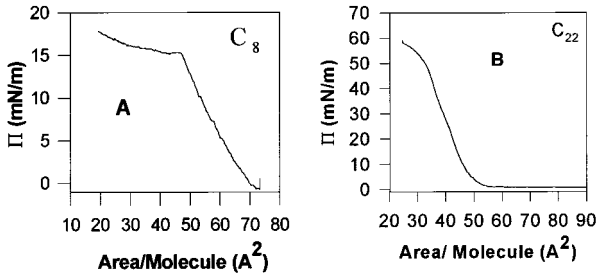

Figure 6. Surface pressure/surface area isotherm at 21 °C of (A) C_8 chromophore **(1d)**, (B) C_{22} chromophore **(1e)**

at 0.40 nm^2 appears at low temperatures and longer delay times (Figure 4B).

The collapse at the higher pressures involves the aggregation of the material in creases parallel to the barrier of the trough. These aggregates can be transferred as Langmuir−Schaeffer (horizontal liftoff) films onto hydrophobic glass slides. Figure 5 shows fluorescent traces observed in a microscope. The separation between the creases is not uniform and varies from dozens to hundreds of microns.

The octyl (**1d**) and docosyl (**1e**) analogues behave roughly in the same way as the hexadecyl derivative (**1a**) does (Figure 6). However, the collapse pressures are different. The C_{22} layer is much more sturdy and collapses at a pressure of ∼50mN/m, while the C_8 layer is rather loose and breaks down at a low pressure of 15mN/m.

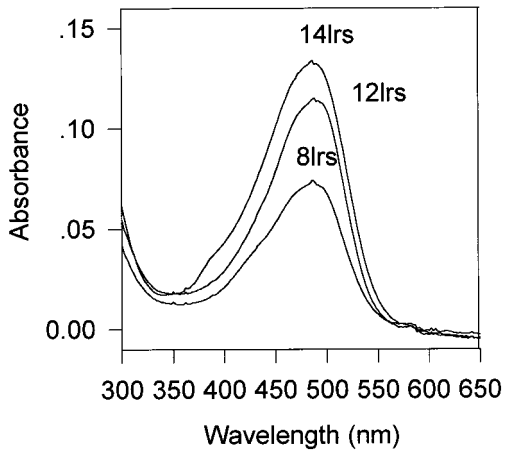

Figure 7. UV−vis spectra of Y-type LB films of **1a** (no spacer), deposited at 20 mN/m, at 21 °C, applying 20 min relaxation of the Langmuir film before deposition. 8, 12, and 14 layers are shown.

TABLE 1: LB Deposition Conditions (temperature and delay time), Transfer Ratios, and Absorption Maxima Wavelengths

deposition conditions				results	
surface pressure (mN/m)		T (°C)	delay time (min)	transfer ratio, τ	absorption maxima (nm)
π_1	20	22	30	0.78−0.88	484
π_2	30	22	90	1−1.15	350/470/501
π_3	28	13	30	0.85−0.95	487
π_4	35	13	90	1−1.15	350/470/501

The surface behavior of **(1a)** on an aqueous solution of cadmium chloride (which is used for the alternate LB films involving cadmium stearate) is essentially the same as described above for pure water.

LB Films. We are mostly interested here in alternate chromophore−spacer LB films (for their NLO behavior). However, we deposited simple (Y-type) LB films of **(1a)** by itself, for purposes of comparison to the results of Rutkis et al.,[6] as well as a reference for the alternate films.

The UV−vis absorbance spectra of these films are shown in Figure 7. They are very similar to the s-polarized spectra reported by Rutkis.[6] The maximum is at ∼480 nm and it is clear, especially for the 8 layers, that this is a convoluted band, with at least two main contributions.

In the case of alternate films we investigate various conditions for their deposition onto glass substrates (Table 1). The UV−vis spectra indicate a uniform transfer of **(1a)** with a high transfer ratio, which depends somewhat on the deposition conditions. A longer curing time after the spreading of the material on the trough allows deposition at higher pressures (30 mN/m and above). The transfer ratios for LB films deposited at these higher pressure (π_2, π_4 points) are 1 ± 0.1, while they are 0.8 ± 0.1 for LB films obtained at lower pressures, and 30 min relaxation (π_1, π_3 points).

A linear dependence of the optical density of the absorption band maximum versus the number of layers is observed for all cases (Figure 8).

The UV−vis spectra of alternate LB films obtained at point π_1 (low deposition pressure) are shown in Figure 9. One peak at 484 nm is observed nearly at the same position seen in a dichloromethane solution (486 nm). The half width at half-maximum (HWHM) of the peak is 39 nm, considerably broader than the absorption band in solution (HWHM = 24 nm in CH_2-

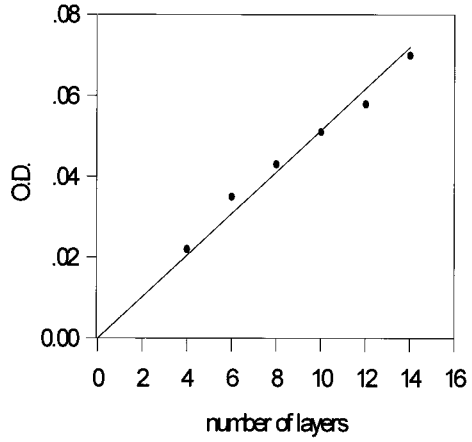

Figure 8. Optical density at 483 nm vs number of layers for LB films of compound (**1a**) deposited 40 min after spreading at 19 mN/m and at 22 °C.

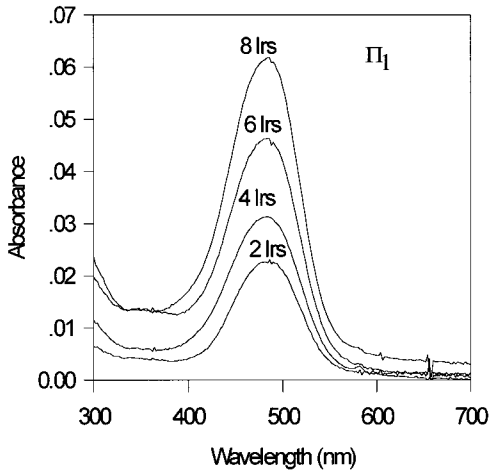

Figure 9. UV−vis absorption spectra of alternate LB films of **(1a)** deposited at the surface pressure π_1.

Cl_2). Similar results are obtained at π_3 where the maximum of the absorption is shifted slightly to 487 nm with a 41 nm HWHM.

The absorption spectra of LB films deposited at points π_2 and π_4 (high deposition pressures) are presented in Figure 10. These spectra differ significantly from those obtained for films transferred at the lower pressures π_1 and π_3. The spectra exhibit a clear dual peak structure. A third very weak feature is seen at a lower wavelength, ~370 nm. Deconvolution using GRAMM32 (Galactic) gives two main log-normal shaped components at 470 and 501 nm. The results are summarized in Table 1.

A series of polarized UV absorption spectra of the LB films are recorded at different incident angles of the light with respect to the film ($\alpha = 30°$, 45°, and 60°). The band intensities for p (parallel to the plane of incidence) and s (perpendicular to the plane of incidence) polarization, I_p and I_s, are obtained from the polarized absorption spectra after baseline correction. The analysis of the polarized spectra is based on the dichroic relation

$$(I_p/I_s)/(I_{0p}/I_{0s}) = [1-10^{-A_p}]/[1-10^{-A_s}] = 1 + (2ctg^2\phi - 1) \times (1 - \cos^2\alpha)$$

with I_p and I_s being the intensity of the transmitted s and p components, respectively. I_{0p} and I_{0s} are the intensity of the incident light at these polarizations, $A_{(p\ and\ s)}$ is the corresponding optical density, ϕ is the tilt of the transition dipole with respect to the normal to the film, and α is the angle of incidence of the

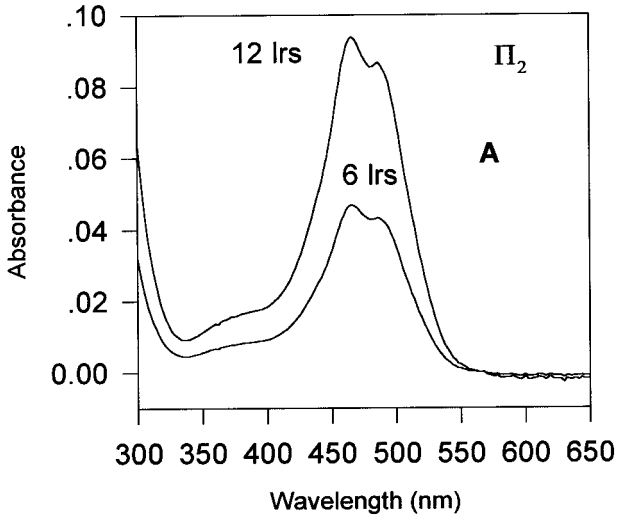

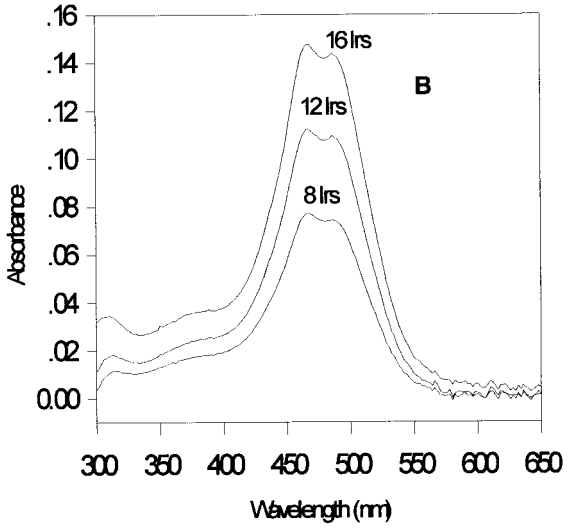

Figure 10. UV−vis absorption spectra of alternate LB films of **(1a)** at different deposition conditions: (A) π_2, (B) π_4.

light with respect to this normal. We assume that all azimuthal angles (with a fixed angle, ϕ, between the transition dipole and the normal to the surface) are equally probable.

In compound **(1a)** the main contribution to the transition dipole lies essentially along the major axis of the molecule. This is inferred from the D−bridge−A structure of the chromophore and is confirmed by quantum mechanical calculations, using the *N*,*N*-dimethylamino analogue of **1** as a model. Calculations of the spectra are performed using B3LYP 6-31G(d) TD/RHF 6-31G(d,p) model chemistry.[8] Whereas geometry optimization at the RHF 6-31G(d) level leads to a geometry close to that found by X-ray diffraction,[9] a reasonable agreement with experimentally observed spectra is achieved only using the DFT time-dependent method.[10] Three singlet long wavelength transitions are calculated for an isolated molecule: 393 nm (f ~ 0), essentially the HOMO^{1-} → LUMO transition; 387 nm (f = 0.81), essentially the HOMO → LUMO transition; and 369 nm (f = 0.15), the HOMO → LUMO^{1+} transition. The value of 387 nm is in good agreement with the wavelength of the intense absorption band expected in a vacuum (397 nm) on the basis of an extrapolation from solvatochromic shifts of spectra measured in solution.[11] This intense absorption band has a charge transfer nature and its position is strongly dependent on the polarity of the surroundings.[12] Since only one intense transition in the visible range is predicted, we might attribute

TABLE 2: Calculated Transition Dipole Moments of the Main Contributions to the Spectrum of (1)

component transition	*X* calc/normalized	*Y* calc/normalized	*Z* calc/normalized
1	−0.078/−0.998	−0.0002/−0.0025	0.0047/0.06
2	−3.21/−0.9999	0.01490/0046	0.0055/0.0017
3	1.343/0.986	0.2244/0.165	−0.014/−0.01

[a] The transition dipoles given here are those starting from the ground vibrational state. Given are also the values normalized to unit length transition dipoles. *x* lies along the largest length of the chromophore (approximately along its long axis), *y* is normal to it in the plane of the molecule, and *z* is normal to the molecular plane.

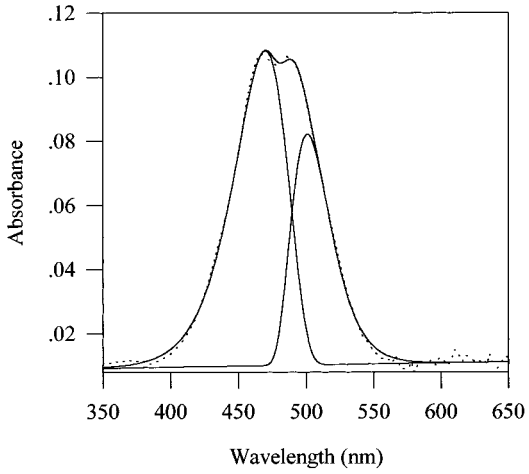

Figure 11. Deconvolution of the absorbance spectrum of a 12-layer LB film of (**1a)** deposited at a high surface pressure.

both intense components in our spectra to the same transition, stemming from either two different molecular conformations or two molecular orientations. The third weak component can stem from the third transition (HOMO → LUMO^{1+}). This transition, as shown by the calculation, involves only a minor degree of charge transfer and is thus less sensitive to the polarity of surroundings, or to the conformer geometry. This assumption is confirmed also by comparing the calculated and experimental transition dipole moments (Table 2). Table 2 gives the components of the transition dipoles of the main transitions contributing to the spectral features listed in Table 1.

Applying the theoretical dichroic ratio to the single (albeit wide) band acquired at the low deposition pressures (π_1 and π_3) we obtain a molecular tilt angle of 39°.

Polarized spectra of LB films deposited at conditions π_3 and π_4 were first deconvoluted into the two components (470 and 501 nm) and then analyzed for their polarization dependence. (Figure 11). The signature at about 370 nm is too weak to be analyzed in a similar fashion.

Both bands are stronger in s-polarization. The dependence of $I_p/I_s - 1$ on the square of the cosine of the angle of incidence for both bands is shown in Figure 12. The tilt angles of the transition moments for characteristic curves at 470 and 501 nm are found to be 40° and 44°, respectively.

Note that though all the three transitions in Table 2 lay predominately along the major chromophore axis, transition 2 is more so, compared to the two other transitions. From this table we can calculate the angles between the three transitions dipoles. They turn out to be: 3.6° between transition dipole 1 and 2, 9.9° (actually 170.1° as dipole 3 is approximately antiparallel to 1 and 2) between dipole 2 and 3, and between dipoles 1 and 3. This situation is described schematically in Figure 13.

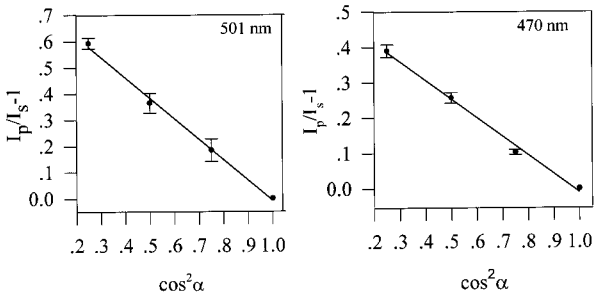

Figure 12. Analysis of polarized UV−vis absorbance spectra of LB films of compound **(1)**. α is the angle of incidence.

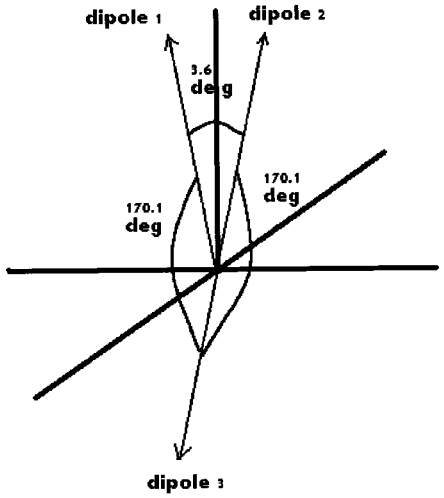

Figure 13. Orientations of the transition dipoles for the ground-state transitions of model compound (**1**).

The structure in the film provides a local environment different than that sensed by the molecule in the solution from which it was deposited. This is manifested in the change of the UV−vis absorption spectrum of the chromophore. In the LB film the second, shorter wavelength transition, at 470 nm, is enhanced. Correspondingly, the spectrum changes from one peak centered at 487 nm (in dichloromethane), to two clear spectral peaks. As shown above, the angle between the (absolute values of the) transition dipoles of the two main transitions in Table 2 is calculated to be ∼10°. This is in a reasonable agreement with the analysis of our variable angle polarized spectrum measurements, that yield an angle difference of 4° between the two main bands. However, the relative intensity of the 470 nm band in the LB film compared to the predicted relative intensity of transition 3 or 1 (Table 2) is too large to be explained by an aligning effect of the surface alone. Solvent effects may play a role, as the chromophore possesses large dipole moments (in the ground and excited states[12]), and will interact differently with the solvent and with the different surrounding in the film.

Alternatively, the two bands in the spectrum can be associated with the same transition in two different conformers, rather than two different transitions of the molecule. In support of this conclusion we carried out semiempirical AM1 calculation for **1a** and found several local energy minima differing by not more than 11 kcal/mol. Two conformers with the largest energy difference of 10.7 kcal/mol are presented in Figure 14. Interestingly, the difference in the position of the long wavelength absorption maxima for both conformers is as large as 14 nm (calculated using the ZINDO method for the AM1 optimized geometries[8]). Thus, the absorption maximum of **1a** is strongly dependent on the value of the twist angle between the dialkylamino group and the phenyl ring. Obviously, several conforma-

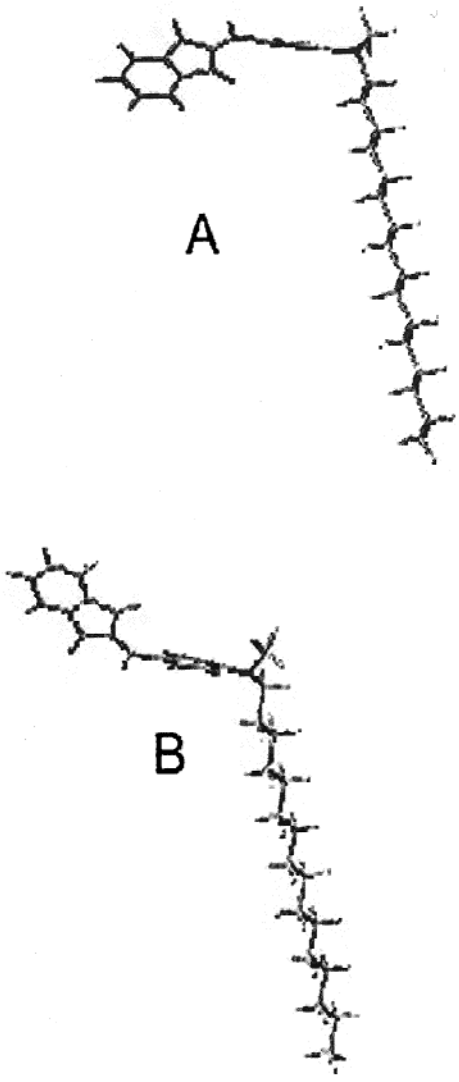

Figure 14. Two conformations of (**1a**) corresponding to two local minima: (a) dihedral angle $C_{16}H_{33}CH_3N$/phenyl 27°, energy −252.097 au, λ_{max} = 327 nm (ZINDO//AM1); (b) dihedral angle $C_{16}H_{33}CH_3N$/phenyl 47°, energy −252.115 au, λ_{max} = 343 nm (ZINDO//AM1).

tions with different twist angles are possible in LB films of **1a** since the energy of the van der Waals interaction between the long alkyl chains could exceed the energy loss owing to the diminished conjugation between the dialkylamino group and the accepting indandione moiety in the twisted conformations. Thus we conclude that different conformers can indeed be responsible for the split spectra we observe in the LB films.

Rutkis et al.,[6] studying a related amphiphile, with the same chromophore, also observed changes in the spectrum in the Langmuir film and the LB films, compared to solution (where a single peak at ∼475 nm was observed). Specifically they deconvoluted their spectra into two components, at ∼455 and 505 nm, with relative intensities rather similar to ours. In addition, for higher pressures they observed another peak emerging at ∼395 nm, which they assign to a H-aggregate.[12] We might have seen only a hint of this feature in our spectra. Rutkis et al. attribute the 455 nm peak to a $S_0 \rightarrow S_1$ molecular transition and the 505 nm peak to a j-aggregate. However, one should note that in contradiction to this, solution spectra of **1**, according to our experiments, are independent of concentration up to 2×10^{-2} M.

One should bear in mind that the molecule investigated by Rutkis et al.[6] is different than the one studied here. The alkyl

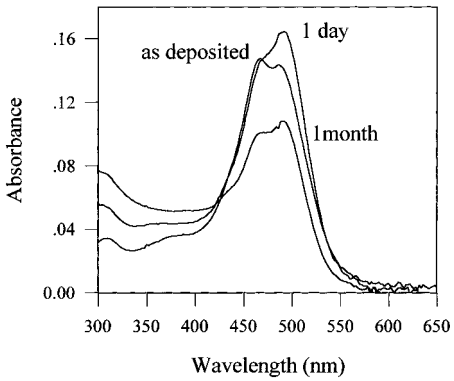

Figure 15. Time-dependent changes in the absorption spectrum of 16-layer LB films of **(1a)** deposited at π_4 conditions.

chain in **1c** is attached to the indandione moiety, while in derivative **1a** it is attached to the amino group. Obviously, the degree of conjugation between the donor and acceptor moieties will be much less affected by conformer formation in the case when a long chain substituent is attached to the rigid benzene ring rather than to the flexible amino group. This difference can also bring about changes in the packing of the molecules and their possible orientations with respect to the surface in the trough and in the LB film. In fact, while Rutkis et al.[6] prepared Y-type LB films on hydrophilic quartz substrates, we needed hydrophobic substrates to obtain reasonably stable multilayer films. This difference makes sense on the basis of the different molecular structures. In derivative **1c**, studied in ref 6, the hydrophilic amino group is rather exposed and can approach hydrophilic (and hydrogen bonding) surfaces. In comparison, in our compound (**1a**) the amino group is blocked by the bulky and hydrophobic C_{16} chain, while the indandione moiety allows for only weak interactions with glass or quartz.

The LB films we deposit on glass deteriorate within a few days, as shown in Figure 15. However the two main peaks are still observable at the same positions.

Similar experiments carried out for the C_8 and the C_{22} long-chain derivatives **1d** and **1e**, instead of the C16 chain, show that in both of these cases the transfer ratios are rather poor, 0.6−0.7, and the LB films are less stable.

SH Generation Measurements. The SH signal obtained from the LB films is characterized by fringes resulting from the interference of SH signals generated by the films on both sides of the glass substrate, with a null signal at 0° and a two-sided symmetry around it (Figure 16). The incidence angles of the minima and maxima are determined by the thickness and coherence length of the glass substrate. The difference of the path length between the peaks is in agreement with the coherence length $\lambda/2\Delta n$, where Δn is the difference of the refractive index between the fundamental and the SH.

In a few cases the SH signal was quadratic in the number of layers deposited in the LB film. However, often this quadratic dependence is not observed, indicating a poor quality of the LB films.

The SHG signals of two representative Y-type LB films (4 and 8 layers) were also checked, and found to be negligible—not more than twice that of the bare substrate, which is typically at least 30-fold weaker than the alternate LB films.

Analysis of the SHG fringe pattern can be performed to yield an effective $\chi^{(2)}$ parameter for the thin film, as well as the molecular β value and orientation. The procedure has been described in the literature,[14] whereby the SHG response is measured for the film under at least two different polarization conditions, and compared with the SHG of a known standard.

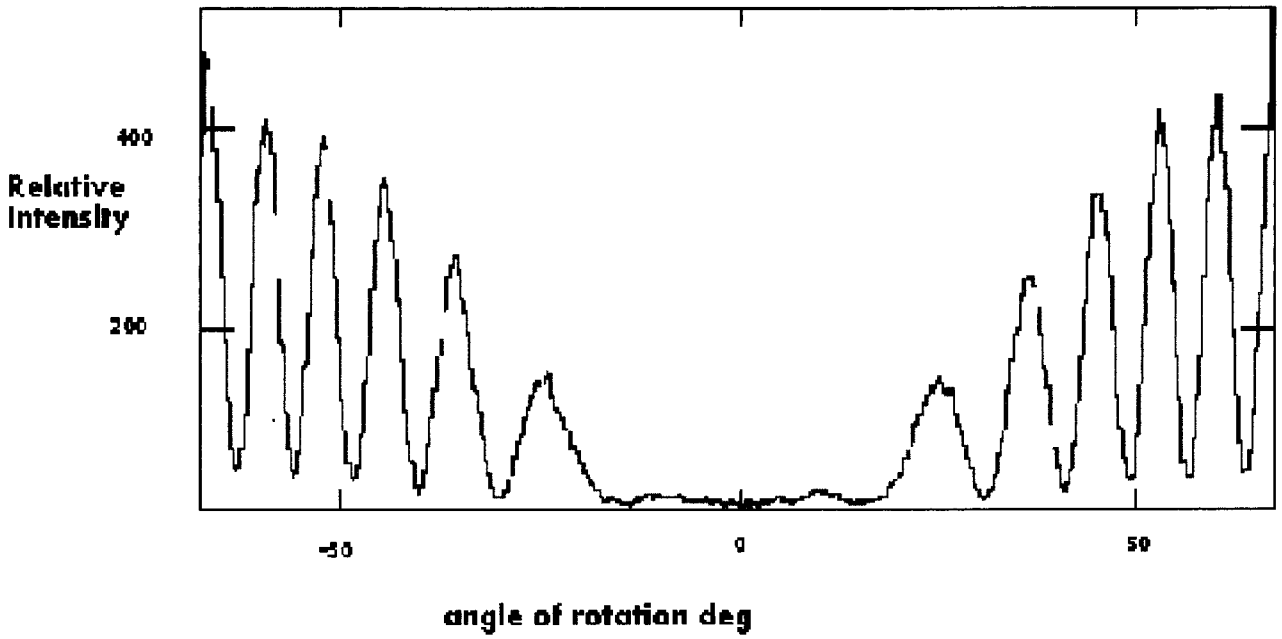

Figure 16. SH generation by a LB film of (**1a**). 8 layers.

The second harmonic field (proportional to the square root of the signal) is a linear combination of the two symmetry-allowed surface susceptibility coefficients, $\chi^{(2)}_{zzz}$ and $\chi^{(2)}_{yzy}$, whose prefactors are known as the nonlinear Fresnel factors.[15] In our case it is simplest to use the bare substrate as the reference, with $\chi^{(2)}_{yzy} = 2.7 \times 10^{-17}$ esu/cm^2.[16] Using this reference, we deduce that for the LB film with 4 layers on each side of the substrate the effective surface susceptibilities (of each side of the film) are approximately $\chi^{(2)}_{zzz} = 2.5 \times 10^{-15}$ esu/cm^2 and $\chi^{(2)}_{yzy} = 1.1 \times 10^{-15}$ esu/cm^2. Considering that the film thickness is about 4 $\times 10^{-7}$ cm, this value is equivalent to a bulk susceptibility of $\chi^{(2)}_{zzz} = 6 \times 10^{-9}$ esu/cm^3, which is several times higher than quartz.

The SH signal for p-polarized input is about 4 to 5 times stronger than for s-input. From the ratio between the signals in the two polarizations, the average orientation of the long axis of the NLO chromophore with respect to the surface normal can be determined,[17] provided the refractive index of the LB film is known (or assumed). The observed polarization ratio is found to give an orientation of 44 $\pm$ 3 degrees.[18] This is in agreement with the tilt angle we evaluate from the polarized absorbance spectra.

The corresponding short chain substituted derivative, **1b**, has been reported to exhibit a zero frequency hyperpolarizability of $\beta_0 = 38 \times 10^{-30}$ esu.[19] We emphazise that the specific molecule studied here is only a convenient model system. We are presently studying other related chromophores that have a much higher NLO activity.

Conclusions and Summary

In this report we discussed the surface behavior of a model NLO choromophore amphiphile based on an acceptor−bridge−donor structure, and the properties of LB films formed from it. The bottom line is that such molecules can form NLO active (alternate) LB films within which the chromophores have a definite orientation with respect to the surface. Both polarized UV−vis absorbance spectra and SH measurements support this conclusion and yield an angle of 40−44° with respect to the surface normal for the transition dipoles of the molecular transitions of this chromophore (lying predominately along the major axis of the chromophore).

The structure within the LB films is affected by the position of the alkyl chain in the amphiphile, as is seen by a comparison of our results with those of Rutkis et al.[6] While we require hydrophobic substrates to form reasonably stable multilayer LB films of compound **1a**, derivative **1c** readily forms Y-type layers on quartz.[6]

In addition, while the transition dipoles of the short wavelength band (455 nm for **1c**[6] and ~470 nm for **1a**) are nearly similarly aligned in the LB films, (42°−52° and 40°−44°, respectively), the orientation of that of the 505 nm band is different (69°−85° for **1c**[6] and ~44° for **1a**).

We find that the two main spectral bands observed in the LB films, and which can be deconvoluted from the solution spectra can be assigned to two nearly (antiparallel) intrinsic molecular transitions, or to transitions associated with different conformers of the molecule. The precise position and intensity of the transitions are affected by the immediate environment of the molecule, which is very different in the LB film than in solution.

Furthermore, the structure of the films strongly depends on the hydrophobic alkyl long-chain used to impart amphiphilic properties to the chromophore-bearing molecule. C_{16} seems to be, more or less, the optimal length. C_{22} is too stiff, and C_8 is too floppy to be picked up as stable multilayer LB films.

2-(*p*-*N*-Hexadecyl-*N*-methylamino)benzylidene-1,3-indandione (**1a**), which we studied here, is a prototype molecule, a model system, for designing strong NLO acitve molecules that can be deposited in stable, multilayer LB films. New derivatives of this basic theme, with much higher expected NLO properties are now under consideration in our lab. Such molecules are interesting from many different aspects: from the synthetic point of view, as they involve several active functional groups, from the perspective of their physical properties (optical, spectroscopical, and packing vs structure), as models for yet more complex molecules, and for their potential use in miniaturized devices.

Acknowledgment. We acknowledge the support of the Israel Ministry of Science.

References and Notes

(1) *Molecular Nonlinear Optics: Materials, Physics and Devices;* Zyss, J., Ed.; Academic Press: Boston, 1994; Eisenthal, K. B. *Chem. Rev.* **1996**, *96*, 1343.

(2) Nalwa, H. S.; Seizo, M. *Nonlinear Optics of Organic Molecules and Polymers*; CRC Press: Boca Raton, FL, 1994.

(3) Blanchard-Desce, M.; Alain, V.; Bedworth, P. V.; Marder, S. R.; Fort, A.; Runser, C.; Barzoukas, M.; Lebus, S.; Wortmann, R. *Chem. Eur. J.* **1997**, *3*, 1091; Marder, S. R.; Tiemann, B. G.; Friedli, A.; Yang, E.; Chang, L. *Nonlinear Optics* **9**, *213*, 1995.

(4) Girling, I. R.; Cade, N. A.; Kolinsky, P. V.; Jones, R. J.; Peterson, I. R.; Ahmad, M. M.; Neal, D. B.; Petty, M. C.; Roberts, G. G.; Feast, W. J. *J. Opt. Soc. Am. B* **1987**, *4*, 950; Zyss, J. *J. Mol. Electronics* **1985**, *1*, 25.

(5) Gulbinas, V.; Kodis, G.; Valkunas, L. *J. Phys. Chem*. **1996**, *100*, 19441; Jursenas, S.; Gulbinas, V.; Gruodis, A.; Kodis, G.; Kovalevskij, V.; Valkunas, L. *Phys. Chem. Chem. Phys*. **1999**, *1*, 1715.

(6) Rutkis, M. A.; Wistus, E.; Lindquist, S. E. *SPIE* **1997**, *2968*, 34.

(7) Agranat, I. *Isr. J. Chem*. **1969**, *7*, 89.

(8) Frisch, M. J.; Trucks, G. W.; Schlegel, H. B.; Scuseria, G. E.; Robb, M. A.; Cheeseman, J. R.; Zakrzewski, V. G.; Montgomery, J. A., Jr.; Stratmann, R. E.; Burant, J. C.; Dapprich, S.; Millam, J. M.; Daniels, A. D.; Kudin, K. N.; Strain, M. C.; Farkas, O.; Tomasi, J.; Barone, V.; Cossi, M.; Cammi, R.; Mennucci, B.; Pomelli, C.; Adamo, C.; Clifford, S.; Ochterski, J.; Petersson, G. A.; Ayala, P. Y.; Cui, Q.; Morokuma, K.; Malick, D. K.; Rabuck, A. D.; Raghavachari, K.; Foresman, J. B.; Cioslowski, J.; Ortiz, J. V.; Baboul, A. G.; Stefanov, B. B.; Liu, G.; Liashenko, A.; Piskorz, P.; Komaromi, I.; Gomperts, R.; Martin, R. L.; Fox, D. J.; Keith, T.; Al-Laham, M. A.; Peng, C. Y.; Nanayakkara, A.; Challacombe, M.; Gill, P. M. W.; Johnson, B.; Chen, W.; Wong, M. W.; Andres, J. L.; Gonzalez, C.; Head-Gordon, M.; Replogle, E. S.; Pople, J. A. *Gaussian 98*, Revision A.9; Gaussian, Inc.: Pittsburgh, PA, 1998.

(9) Magomedova, N. S.; Kolninov, O. V.; Ruchadze, Y. G.; Zvonkova, Z. V. *Zh. Fiz. Khim*. **1975**, *49*, 1322; Magomedova, N. S.; Zvonkova, Z. V. *Kristallografiya* **1978**, *23*, 281; Khodorkovsky, V.; Mazor, R.; Ellern, A. *Acta Crystallogr. C* **1996**, *52*, 2878.

(10) Bauernschmitt, R.; Ahlrichs, R. *Chem. Phys. Lett*. **1997**, *264*, 573; Casida, M. E.; Jamorsky, C.; Kasida, K. C.; Salahub, D. R., *J. Chem. Phys*. **1998**, *108*, 4439.

(11) Khodorkovsky, V.; Shapiro, L.; Mazor, R.; Rubstein, B.-Z. Submitted for publication.

(12) Jursenas, S.; Gruodis, A.; Kodis, G.; Chachisvilis, M.; Gulbinas, V.; Silinsh, A. E.; Valkinas, L. *J. Phys. Chem. B* **1998**, *102*, 1086.; Jursenas, S.; Gulbinas, V.; Gruodis, A.; Kovalevskij, V.; Valkunas, L. *Phys. Chem. Chem. Phys*. **1999**, *1*, 1715.

(13) Czikkely, V.; Forsterling, H.; Kuhn, H. *Chem. Phys. Lett.* **1970**, *6*, 207.

(14) Kajzar, F.; Messier, J.; Zyss, J.; Ledoux, I. *Opt. Comm.* **1983**, *45*, 133; Rasing, T.; Berkovic, G.; Shen, Y. R.; Grubb, S. G.; Kim, M. W. *Chem. Phys. Lett*. **1986**, *130*, 1; Dentan, V.; Ledoux, I.; Hierle, R.; Zyss, J. *Nonlinear Optics* **1993**, *5*, 407.

(15) Naujok, R. R.; Higgins, D. A.; Hanken, D. G.; Corn, R. M. *J. Chem. Soc., Faraday Trans.* **1995**, *91*, 1411; Guyot-Sionnest, P.; Shen, Y. R. *Phys. Rev. B* **1987**, *35*, 4420.

(16) The calculation has assumed a refractive index $n = 1.4$, typical for organic materials.

(17) Mizrahi, V.; Sipe, J. E. *J. Opt. Soc. Am. B* **1988**, *5*, 660.

(18) If a refractive index $n = 1.5$ is assumed, the resulting tilt angle is changed only to 40 ± 2.

(19) Moylan, C. R.; Twieg, R. J.; Lee, V. Y.; Swanson, S. A.; Betterton, K. M.; Miller, R. D. *J. Am. Chem. Soc*. **1993**, *115*, 12599; Meshulam, G.; Berkovic, G.; Kotler, Z.; Ben-Asuly, A.; Mazor, R.; Shapiro, L.; Khodorkovsky, V. *Synth. Met*. **2000**, *115*, 219.